CSIRO PUBLISHING

Exploration Geophysics, 2012, **43**, 162–170
http://dx.doi.org/10.1071/EG11039

Error analysis of the converted wave deduced by equivalent velocity assumption

Wei Wang[1] Yun Wang[2,4] Junjie Yin[3] Xing Gao[1]

[1]The State Key Laboratory of Resources and Environmental Information System, Institute of Geographic Sciences and Natural Resources Research, Chinese Academy of Sciences, Beijing 100101, China.
[2]Institute of Geochemistry, Chinese Academy of Sciences, Guiyang 550002, China.
[3]China United Coal Bed Methane Co., Ltd., Beijing, 100011, China.
[4]Corresponding author. Email: yunwang@mail.iggcas.ac.cn

Abstract. Based on the assumption of the equivalent velocity and offset, the converted wave travel-time equation, which has a double square root due to the asymmetric ray-path of the down-going *P*-wave and the up-coming *S*-wave, can be transformed into a single square root equation if the common scatterpoint (CSP) gathers are binned. This method simplifies the equation and decreases the errors of converted wave migration transferred by *P*-wave velocity error, compared to the equivalent offset method (EOM) migration proposed by Bancroft, Geiger and Foltinek . In this paper, the errors caused by the introduction of equivalent velocity for the *PS*-wave are analysed in detail. The discrete errors and effects introduced by discretization of the equivalent offset are presented, and finally the conditions for applying CSP gathers for *PS*-wave processing under the control of reasonable error limits are derived.

Key words: converted wave, EOM, equivalent offset, equivalent velocity, error analysis.

Received 26 July 2011, accepted 17 March 2012, published online 16 May 2012

Introduction

The equivalent offset method (EOM) migration of the *P*-wave was first brought forward by Bancroft and Geiger (Bancroft and Geiger, 1996; Bancroft et al., 1994) and was subsequently applied to the converted wave migration (Bancroft and Wang, 1994; Bancroft et al., 1995, 1998; Li and Bancroft, 1997). The converted wave migration method based on isotropic media is different from the method by Dai and Li (2007), which is based on anisotropic media and includes anisotropy parameters used to calculate the travel time. The fundamental procedure of the converted wave EOM method consists of three steps. The first step is to obtain a *P*-wave migrating velocity model from common scatterpoint (CSP) gathers; the second step is to obtain the *P*- to *S*-wave velocity ratio from *PS*-wave CSP gathers binned with a constant velocity ratio; and the third is to repeat the second step of migration until a reasonable velocity ratio model is reached. Wang et al. (1996) tested the velocity sensitivity by numerical simulation and concluded that the common conversion scatterpoint gathers and velocity analysis are fairly insensitive to the velocity error.

The CSP gathers for the converted wave, which are obtained by the method mentioned above, are affected by the accuracy of *P*-wave velocity. It is difficult to obtain accurate *P*-wave velocity in the case of complex structures, such as steep dip sub-surfaces and significant lateral velocity variation, especially if the seismic data are characterised by low signal-to-noise ratios (SNR) or weak reflections. The simplified converted wave CSP gathers can be calculated without the *P*-wave velocity by the introduction of an equivalent *PS*-wave velocity. It is worth noting that an error could be introduced by the assumption of an equivalent *PS*-wave velocity, and the suitable conditions for using the method are determined by the velocities and ray-path.

Error analysis of converted wave in CSP gathers and its applicable conditions

Theory of converted wave imaging

Figure 1 shows the schematic diagram of the equivalent offset (Bancroft and Geiger, 1996), where **S** is the source point, **R** is the receiver point, CSP is the common scatterpoint, CMP is the common midpoint, **O** is the ground projection position of the scatterpoint, **E** is the collocated position of the equivalent source and receiver point, Z_0 is the scatterpoint depth, x is the distance from CMP to the projection point (**O**), h is the half-offset, h_e is the distance between **E** and **O**, which defines the equivalent offset, h_s is the distance from source (**S**) to the projection point (**O**), and h_r is the distance from the receiver (**R**) to the projection point (**O**).

The total travel time is expressed by $T = T_p + T_s$, when the wave propagates from source **S** to the scatterpoint with *P*-wave velocity, and then from the scatterpoint to the receiver **R** with the *S*-wave velocity.

It is assumed that: (1) *PS*-waves propagate at a equivalent velocity (V_e) from the source to the scatterpoint, and then to the receiver, and its travel time will be equal to the sum of time that the *P*-wave travels from the source to the scatterpoint at the *P*-wave velocity (V_P), and the *S*-wave travels from the scatterpoint to the receiver at the *S*-wave velocity (V_S); and (2) the virtual source and receiver located on the same position (**E**) with the same travel time at the velocity of V_e.

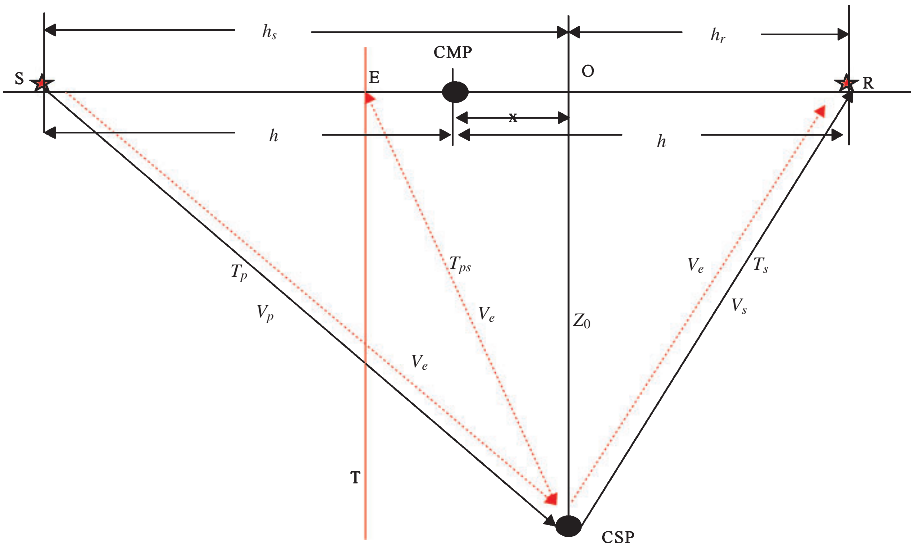

Fig. 1. Schematic diagram of equivalent offset (h_e), in which the broken-arrow lines indicate that the wave propagates at equivalent velocity V_e from the source to the scatterpoint (CSP), then to the receiver (R). Other parameters are described in the text.

Based on the first assumption, we have the following equation:

$$\left[\left(\frac{Z_0}{V_P}\right)^2+\frac{(x+h)}{V_P^2}\right]^{\frac{1}{2}}+\left[\left(\frac{Z_0}{V_S}\right)^2+\frac{(x-h)^2}{V_S^2}\right]^{\frac{1}{2}}$$
$$=T_{p+s}=\left[\left(\frac{Z_0}{V_e}\right)^2+\frac{(x+h)^2}{V_e^2}\right]^{\frac{1}{2}}+\left[\left(\frac{Z_0}{V_e}\right)^2+\frac{(x-h)^2}{V_e^2}\right]^{\frac{1}{2}} \tag{1}$$

where, V_P is the migration velocity of the *P*-wave, and V_S is the migration velocity of the *S*-wave. It is obvious that the equation 1 is a double square root (DSR) equation with equivalent velocity and equivalent offset parameters.

Based on the second assumption, we have the following equation:

$$T_{p+s}=2\left[\left(\frac{Z_0}{V_e}\right)^2+\frac{h_e^2}{V_e^2}\right]^{\frac{1}{2}}. \tag{2}$$

Combining the two equations above, the following equation can be deduced,

$$2\left[\left(\frac{T_0}{2}\right)^2+\frac{h_e^2}{V_e^2}\right]^{\frac{1}{2}}=\left[\left(\frac{T_0}{2}\right)^2+\frac{(x+h)^2}{V_e^2}\right]^{\frac{1}{2}}+\left[\left(\frac{T_0}{2}\right)^2+\frac{(x-h)^2}{V_e^2}\right]^{\frac{1}{2}} \tag{3}$$

where, $T_0/2=Z_0/V_e$.

Equation 3 can be simplified as the derivation by Bancroft et al. (1998) applied in *P*-wave processing. V_p is replaced with a different velocity (see Appendix):

$$h_e^2=x^2+h^2-\left(\frac{2xh}{TV_e}\right)^2 \tag{4}$$

Equation 4 can be re-written as shown in equation 5, which is used to sort converted wave CSP gathers:

$$T=\frac{2xh}{V_e\left(x^2+h^2-h_e^2\right)^{\frac{1}{2}}}. \tag{5}$$

The equation is similar to the *P*-wave equation of (Bancroft et al., 1998), but the V_e has a different value; it is an equivalent *PS*-wave velocity and has a symmetric travel time.

The process to form CSP gathers of converted waves using equation 5 is as simple as forming CSP gathers of the *P*-wave. First, CSP gathers are formed by a given constant velocity, and then velocity analysis will be done on selected CSP gathers to yield a variable velocity model, where new CSP gathers are formed by the variable velocity. Then this process is repeated until the accurate velocity models are reached. Finally, new CSP gathers, which are formed by an accurate velocity model, are used to image the seismic section. It is worth noting that the velocity estimation converges rapidly after the second step, and only two or three iterations are required.

However, it is not possible to find a constant equivalent velocity for different positions of sources or receivers, because it is variable at the same scatterpoint. An error will be introduced when forming CSP gathers of converted waves with a constant V_e, as $V_e\in(V_s, V_p)$, $2V_P/(1+\gamma)$ (see the section 'Discussion on the substitution of $2V_p/(1+\gamma)$') or $3V_p/(1+2\gamma)$ is selected as an approximate substitution to the value of the equivalent velocity, in which $\gamma=V_p/V_s$.

Error analysis deduced by equivalent velocity

Based on the theory of converted wave scatter imaging mentioned above, we assume that the real two-way travel time, in which a wave propagates downwards from the source to the common converted scatterpoint with *P*-wave velocity, and then goes up to the receiver with *S*-wave velocity, and is equal to the travel time that wave propagates along the same paths with equivalent velocity. Obviously, under the above assumption, a part of scattered energy cannot be mapped to its correct position along the scattering wave hyperbola on CSP gathers, when using equivalent velocity, thus, the error is estimated by the proportional error:

$$E = (T_h - T_i)/T_h$$
$$= \left(2\sqrt{(t_0/2)^2 + (h_e/V_e^2)} - \sqrt{Z_0^2 + (x-h)^2}/V_p - \sqrt{Z_0^2 + (x+h)^2}/V_s\right)/2\sqrt{(t_0/2)^2 + (h_e/V_e)^2} \quad (6)$$

where T_h is the travel time along the hyperbola that is formed by a given V_e and t_0, and every (V_e, V_0) indicates a scattering wave hyperbola. V_i is the real travel time.

For a given location of the scatterpoint, P- and S-wave velocity, the true travel time, in which the P-wave propagates from the source to the scatterpoint and the S-wave propagates from the scatter-point to the receiver, is expressed as follows:

$$T_i = \sqrt{Z_0^2 + (x-h)^2}/V_p + \sqrt{Z_0^2 + (x+h)^2}/V_s. \quad (7)$$

By applying T_i to equation 5 (see equations 9 and 10), we derive the equivalent offset h_e. At the same h_e the predetermined travel time is:

$$T_h = 2\sqrt{Z_0^2 + h_e^2}/V_e = 2\sqrt{(t_0/2)^2 + (h_e/V_e)^2}, \quad (8)$$

where the first substitution of equivalent velocity $2V_p/(1+\gamma)$ is selected.

Finally, we derive a proportional error E by equation 6. Figure 2 shows the variety of the proportional error with the half offset h and the CMP to CSP projection point distance x. We conclude that:

(1) The proportional error E increases with half offset h and constant x, but E decreases with increasing h when exceeding the extreme value of E;
(2) The extreme value increases with x;
(3) When x is small, E is not sensitive to h and the error can be ignored.

E is not sensitive to x and varies within a small range for a given value of h. For example, when x is 400 m, with a large offset greater than 1750 m or a small offset less than 900 m, the absolute maximum error E is less than 4%; when x is 1200 m, with a small offset less than 350 m, the absolute maximum error E is less than 4%. The error decreases as the depth of the scatterpoint increases, when given the same parameters of x, h and Ve.

When selecting the second substitution $3V_p/(1+2\gamma)$, similar results (illustrated in Figure 3) can be obtained, but the error values are different.

Given the position of scatterpoint Z_0 (0 m, 1200 m), velocity of P-wave $V_p = 3000$ m/s, equivalent velocity is equal to proximal value $V_e \approx 2V_p/(1+\gamma)$, and $\gamma = V_p/V_s$ (see section 'Discussion on the substitution of $2V_p/(1+\gamma)$'), the real travel time can be expressed as

$$T_i = \sqrt{Z_0^2 + (x+h)^2}/V_p + \sqrt{Z_0^2 + (x+h)^2}/V_s$$
$$= \frac{2}{1+\gamma}\sqrt{\left(\frac{t_0}{2}\right)^2 + \left(\frac{x-h}{V_e}\right)^2} + \frac{2\gamma}{1+\gamma}\sqrt{\left(\frac{t_0}{2}\right)^2 + \left(\frac{x-h}{V_e}\right)^2}. \quad (9)$$

The predetermined travel time equation on CSP gathers is written as

$$T_h = 2\sqrt{(t_0/2)^2 + (h_e/V_e)^2}$$
$$= \sqrt{\left(\frac{t_0}{2}\right)^2 + \left(\frac{x-h}{V_e}\right)^2} + \sqrt{\left(\frac{t_0}{2}\right)^2 + \left(\frac{x+h}{V_e}\right)^2}. \quad (10)$$

Combining equations 9 and 10, the proportional error can be written as:

$$E = (T_h - T_i)/T_h$$
$$= \left(\frac{\gamma-1}{1+\gamma}\sqrt{\left(\frac{t_0}{2}\right)^2 + \left(\frac{x-h}{V_e}\right)^2} + \frac{1-\gamma}{1+\gamma}\sqrt{\left(\frac{t_0}{2}\right)^2 + \left(\frac{x+h}{V_e}\right)^2}\right) \Big/ \left(\sqrt{\left(\frac{t_0}{2}\right)^2 + \left(\frac{x-h}{V_e}\right)^2} + \sqrt{\left(\frac{t_0}{2}\right)^2 + \left(\frac{x+h}{V_e}\right)^2}\right) \quad (11)$$

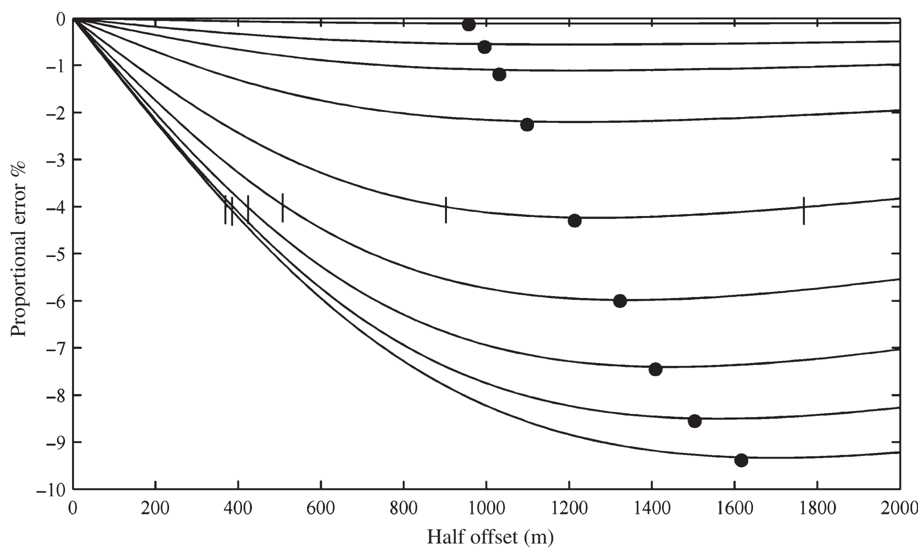

Fig. 2. Curves of proportional error E with half offset h (CMP to CSP projection point distance, from top to bottom $x = 10$, 50, 100, 200, 400, 600, 800, 1000, 1200 m, respectively), in which the black dots note the extreme value of the proportional error curve, and the depth of scatter point is 1200 m.

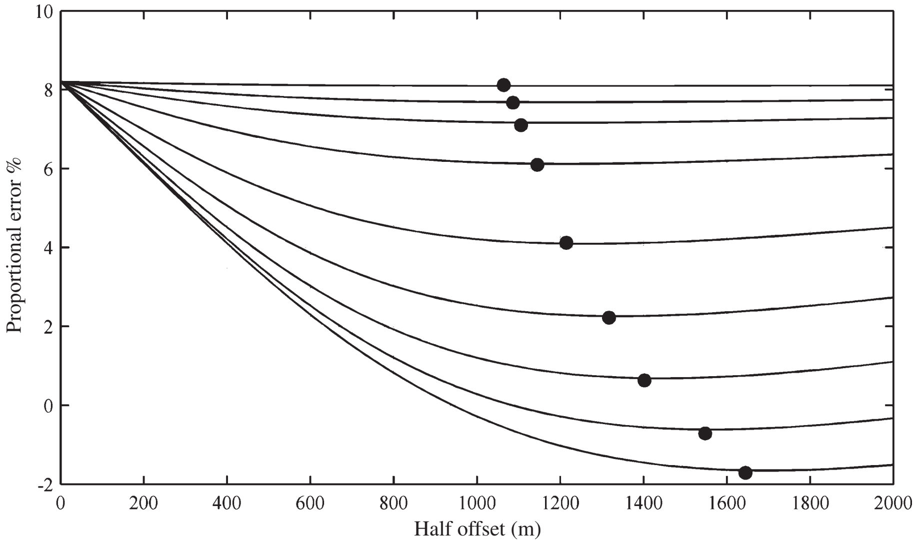

Fig. 3. Curves of proportional error E with half offset h (CMP to CSP projection point distance from top to bottom $x=10$, 50, 100, 200, 400, 600, 800, 1000, 1200 m, respectively) by different equivalent velocity, in which the black dots represent the extreme value of the proportional error, and the depth of scatter point is 1200 m.

Since Poisson's ratio of seismic media generally distributes within the range of [0, 0.5], $\sigma \in [0, 0.45]$ is selected to calculate the corresponding velocity ratio, and $\gamma \in [1.414, 3.317]$ is obtained correspondingly.

The proportional error $\boldsymbol{E}$ increases with the velocity ratio, as illustrated in Figure 4.

E varies around one percent when the receiver is near to source, i.e. h = 10 m. So for the given velocity ratio, if it ranges from 1.5 to 3.0, the input seismic data with a relatively large x and h can be mapped into CSP gathers. But, when there is larger (defined by the user, usually 10%) error generated, the traces will be discarded during forming CSP gathers.

Comparing the equivalent offset geometry of the P-wave (Wei et al., 2007) to that of the converted wave, the different arrival times caused by the up-going wave can be observed. The arrival time of the P-wave is mainly determined by the travelling distance and the velocity of the P-wave, while the equivalent offset of the converted wave is not only determined by the downward P-wave, but also by the up-going S-wave. Therefore a time difference will be introduced if the locations of source and receiver are exchanged for the same x and h, and then the proportional error can be expressed as:

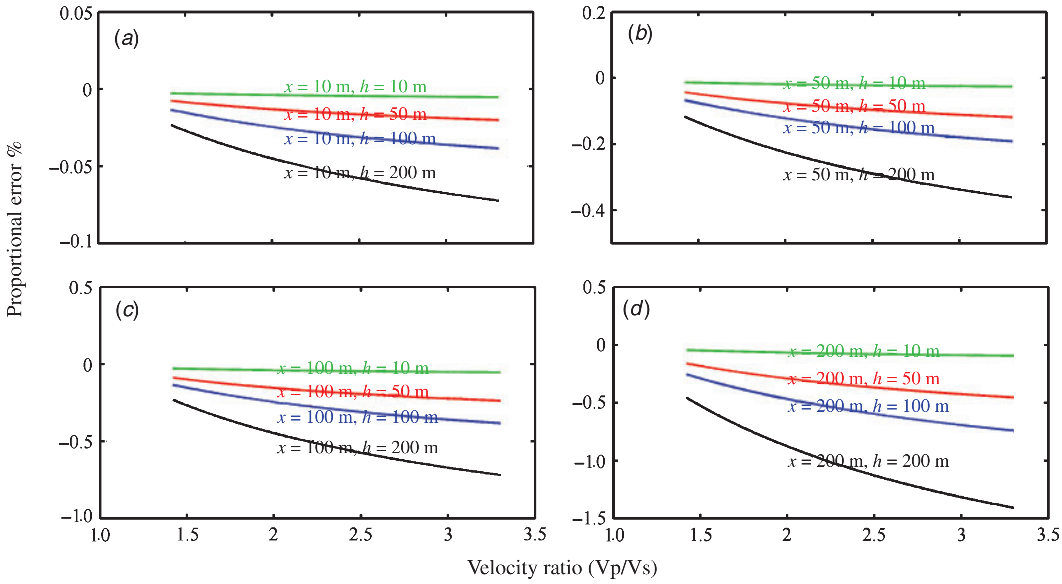

Fig. 4. Variation of proportional error E with velocity ratio γ (in Figure 4*a*, the green, red, blue, and black curves represent $x=10$ m, half-offset $h=10$ m, 50 m, 100 m, 200 m, respectively; Figure 4*b*, 4*c* and 4*d* correspond to the conditions of $x=50$ m, 100 m, and 200 m respectively.)

$$
\begin{aligned}
E &= (T_h - T_i)/T_h \\
&= \left(\left(\frac{\gamma-1}{1+\gamma}\right) \sqrt{\left(\frac{t_0}{2}\right)^2 + \left(\frac{x+h}{V_e}\right)^2} + \frac{1-\gamma}{1+\gamma} \sqrt{\left(\frac{t_0}{2}\right)^2 + \left(\frac{x-h}{V_e}\right)^2} \right) / \\
&\left(\sqrt{\left(\frac{t_0}{2}\right)^2 + \left(\frac{x+h}{V_e}\right)^2} + \sqrt{\left(\frac{t_0}{2}\right)^2 + \left(\frac{x-h}{V_e}\right)^2} \right). \\
&= -\left(\frac{\gamma-1}{1+\gamma} \sqrt{\left(\frac{t_0}{2}\right)^2 + \left(\frac{x-h}{V_e}\right)^2} + \frac{1-\gamma}{1+\gamma} \sqrt{\left(\frac{t_0}{2}\right)^2 + \left(\frac{x+h}{V_e}\right)^2} \right) / \\
&\left(\sqrt{\left(\frac{t_0}{2}\right)^2 + \left(\frac{x+h}{V_e}\right)^2} + \sqrt{\left(\frac{t_0}{2}\right)^2 + \left(\frac{x-h}{V_e}\right)^2} \right)
\end{aligned} \tag{12}
$$

Equation 12 proves that the absolute value of the proportional error is equal to the value before the exchange of the source and receiver. In other words, on CSP gathers the scattered energy deviates from the scatter hyperbola upward and downward, and the deviation increases with the equivalent offset. When binning the CSP gathers with equation 5, the scattered energy of converted waves will show a step-divergence (Figure 5, left) along the scatter hyperbola.

Discrete error analysis

When binning CSP gathers, scattered energy from the same scatter-point are mapped into a CSP gather along a hyperbola. From the scatter hyperbola equation

$$
t = 2\sqrt{\left(\frac{T_0}{2}\right)^2 + \left(\frac{h_e}{V_e}\right)^2},
$$

we can derive the following equation, where Taylor expansion was executed and high-order items were omitted:

$$
\begin{aligned}
t &= t_0 + t(h_e)(dh_e) + \frac{tV_e^4}{2}\left(\frac{dh_e}{V_e^2}\right) + \cdots \\
&\approx 2\sqrt{\left(\frac{T_0}{2}\right)^2 + \left(\frac{h_e}{V_e}\right)^2} \\
&+ \frac{2h_e(dh_e)}{V_e^2\sqrt{\left(\frac{T_0}{2}\right)^2 + \left(\frac{h_e}{V_e}\right)^2}} + \frac{\left(\left(\frac{T_0V_e}{2}\right) - h_e^2\right)\left(\frac{dh_e}{V_e^2}\right)^2}{\left(\left(\frac{T_0}{2}\right)^2 + \left(\frac{h_e}{V_e}\right)^2\right)^{\frac{3}{2}}}.
\end{aligned} \tag{13}
$$

So the discrete error is

$$
\begin{aligned}
E_d &= t - t_0 = \\
&+ \frac{2h_e(dh_e)}{V_e^2\sqrt{\left(\frac{T_0}{2}\right)^2 \left(\frac{h_e}{V_e}\right)^2}} + \frac{\left(\left(\frac{T_0V_e}{2}\right) - h_e^2\right)\left(\frac{dh_e}{V_e^2}\right)^2}{\left(\left(\frac{T_0}{2}\right)^2 + \left(\frac{h_e}{V_e}\right)^2\right)^{\frac{3}{2}}}.
\end{aligned} \tag{14}
$$

When the scatter hyperbola is binned by dh_e (Figure 6*a*), which is equivalent to filtering the input data at a random time sample with a spatial boxcar filter of width dh_e, the higher frequencies are attenuated on the steep part of the hyperbola (Bancroft et al.,1998). The effects of attenuating higher frequencies increases with the hyperbola dip, which enlarges the frequency range. A small dh_e could enlarge the range of higher frequencies, but will increase the memory usage and require an intensive computing time during migration, leaving little for forming CSP gathers.

Figure 6*b* and 6*c* are the frequency spectrum analysed with the corresponding equivalent offset interval 5 m (left) and 2.5 m (right), respectively. Giving an 18 db for the boundary, the

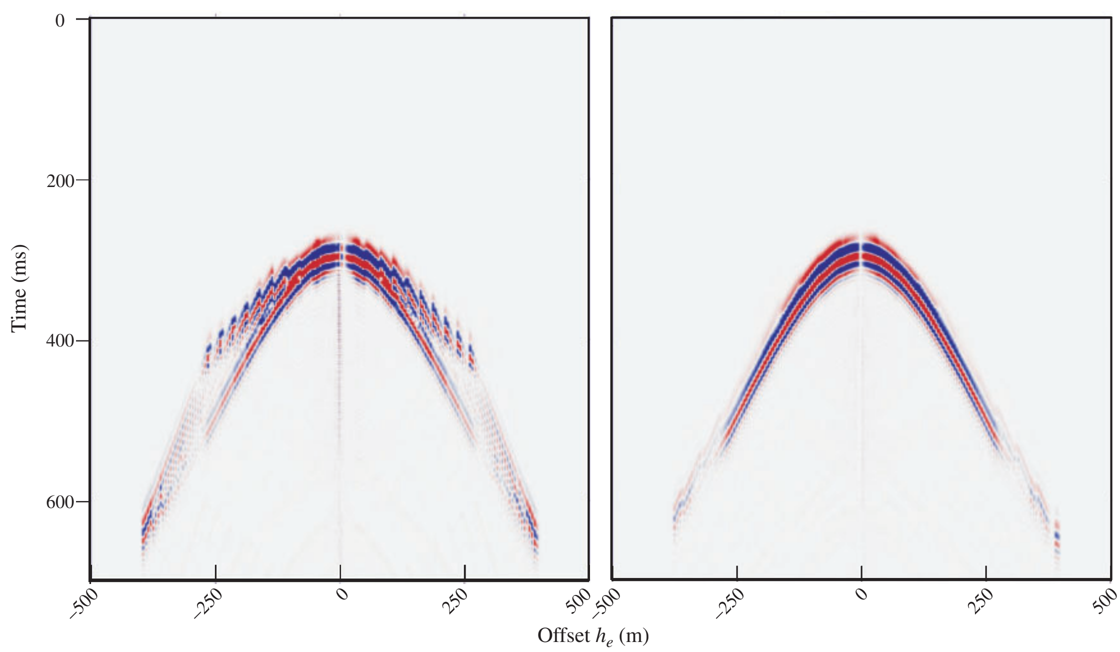

Fig. 5. CSP gather with step-divergence noise (left) and without step-divergence noise (right).

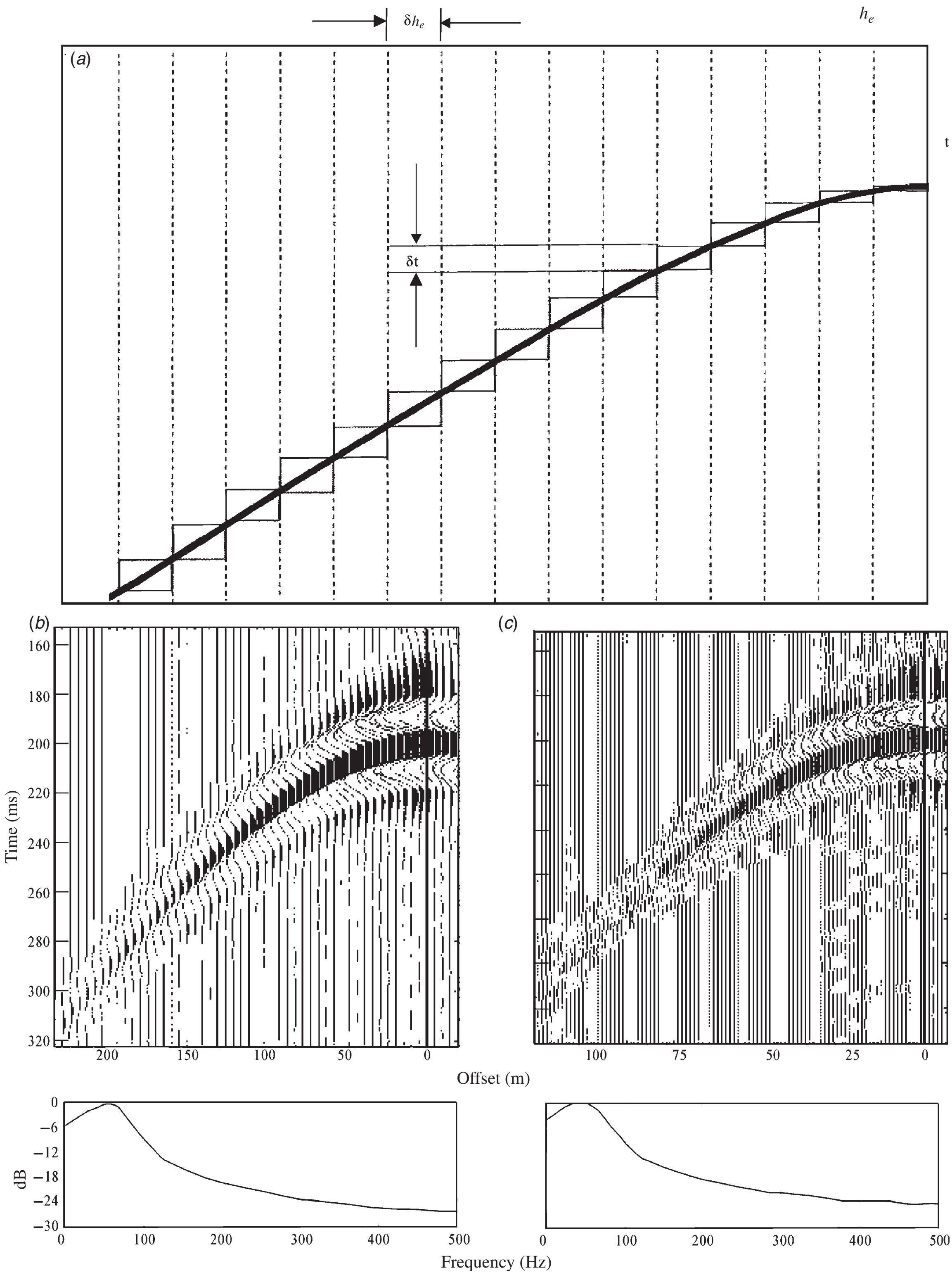

Fig. 6. Effect of equivalent offset discretization. (*a*) Hyperbolic event in a CSP gather with bins of width dh_e (Bancroft et al., 1998); (*b*) frequency spectrum when the equivalent offset interval is set to 5 m; and (*c*) the spectrum with interval equal to 2.5 m.

frequency band range is 1–170 Hz when $dh_e = 5$ m, and 1–200 Hz when $dh_e = 2.5$ m. The large equivalent offset has suppressed the high-frequencies, which have similar properties to a temporal filter attenuating spatially aliased frequencies, as required by the Kirchhoff migration (Bancroft et al., 1998). We recommend that the dh_e is set equal to the half offset h for 2D or 3D *PS*-wave processing, based on our experiments of field seismic data processing.

Applicable conditions

Conclusions can be drawn from the analysis presented above on the equivalent velocity error and discrete error. The step-divergence noise can be ignored and has little effect on the precision of velocity analysis when the location of the source and receiver are exchanged within a small range. However, the noise has a significant effect on the migration process, and is required to be suppressed on CSP gathers of converted waves.

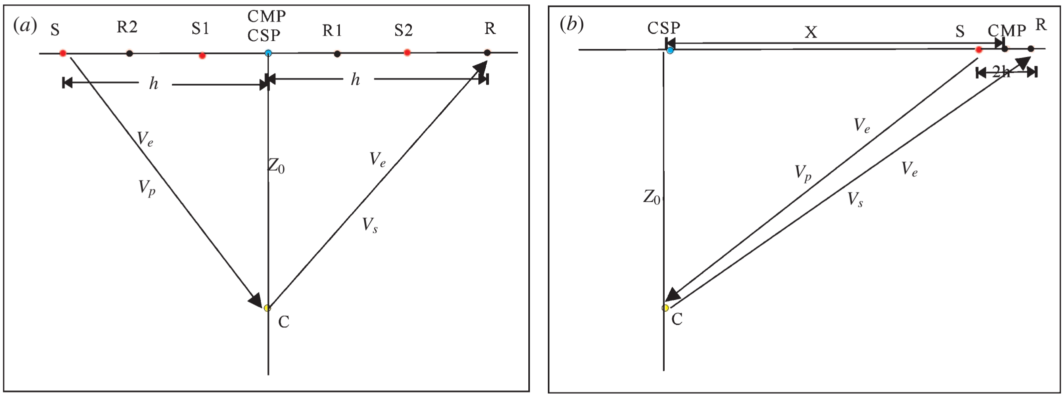

Fig. 7. Approximate value of equivalent velocity $V_e=2V_p/1+\gamma$ in case of (*a*) $x=0$ m or (*b*) $x >> h$, during CMP gathers mapped into CSP gathers at the same surface position.

Since the noise is caused mainly by the velocity difference of the up-going wave and exchange of the source and receiver, in order to improve the SNR, the step-divergence noise was suppressed by sorting input gathers under reasonable conditions, including the exchange of the locations of sources and receivers, and selection of the small offset h and distance x (illustrated in Figure 5, right), during formation of CSP gathers of converted waves.

Discussion on the substitution of $2V_p/(1+\gamma)$

If the positions of CMP and CSP gather are in superposition, namely, $x=0$, or the distance between CSP and CMP is much more than the offset, i.e. $x >> h$ (see Figure 7), then it can be derived that:

(1) When $x=0$ or $x\approx 0$ (Figure 7*a*),

$$SC=\sqrt{h^2+Z_0^2},\quad RC=\sqrt{h^2+Z_0^2}. \tag{15}$$

According to the definition of equivalent velocity and the first assumption, we can have

$$T=\frac{SC}{V_p}+\frac{RC}{V_s}=\frac{SC}{V_e}+\frac{RC}{V_e}. \tag{16}$$

Simplifying

$$\begin{aligned}&\Rightarrow\frac{SC}{V_p}+\frac{SC}{V_s}=\frac{SC}{V_e}+\frac{SC}{V_e}\Rightarrow SC\left(\frac{V_s+V_p}{V_sV_p}\right)\\&=\frac{2SC}{V_e}\Rightarrow V_e=\frac{2V_sV_p}{V_s+V_p}=\frac{2V_p}{1+\gamma}\end{aligned} \tag{17}$$

where

$$SC=\sqrt{(x+h)^2+Z_0^2},\quad RC=\sqrt{(x-h)^2+Z_0^2} \tag{18}$$

(2) Alternatively, when $x>>h$ (Figure 7*b*),

$$SC=\sqrt{x^2+Z_0^2},\quad RC\approx\sqrt{x^2+Z_0^2}, \tag{19}$$

which can be written as

$$SC\approx RC\approx\sqrt{x^2+Z_0^2}. \tag{20}$$

We will still have the approximate result

$$V_e\approx 2\frac{V_p}{1+\gamma}. \tag{21}$$

The CMP gathers data can be mapped into CSP gathers in the same surface position with the same parameter of $V_e=2V_p/1+\gamma$, when $x=0$ (Figure 7*a*) or $x >> h$ (Figure 7*b*).

Conclusions

The introduction of equivalent velocity during converted wave scattering imaging enables development of the equivalent offset migration and simplifies the equation for forming CSP gathers without the *P*-wave velocity calculation. Based on the error analysis discussed above, it is concluded that:

(1) The proportional error E increases with half offset h and the constant CMP to CSP projection point distance x, but E decreases when h is beyond the extreme position of E.
(2) When x is small, E is not sensitive to h and can be ignored.
(3) The proportional error E increases with velocity ratio γ, but it varies within a small range.
(4) The step-divergence noise is mainly introduced by the up-going velocity and exchanging sources and receivers' locations.
(5) The discrete equivalent offset dh_e plays a role of anti-aliases filter.

In summary, equivalent velocity can be applied to bin converted wave CSP gathers according to scatter hyperbola under reasonable conditions. The method also simplifies the next step of velocity analysis and is favoured by the Kirchhoff integral migration.

Acknowledgements

The research is supported by Open Fund (NO.GDL0803) of Key Laboratory of Geo-detection (China University of Geosciences, Beijing), Ministry of Education, National Special Fund (NO. 2011ZX05035–001–006HZ, 2011ZX05035–002–003HZ, 2011ZX05008–006–22, 2011ZX05049–01–02, 2011ZX05019–003), and Natural Science Foundation of China (grant numbers: 41130419, 41074041).

References

Bancroft, J. C., and Geiger, H. D., 1996, Velocity sensitivity for equivalent offset prestack migration: a contrast in robustness and fragility: *CSEG National Convention, Expanded Abstracts*, 149–150.

Bancroft, J. C., and Wang, S., 1994, Converted-wave prestack migration and velocity analysis by equivalent offsets and CCP gathers: *CREWES Research Report*, **6**, 28.1–28.7.

Bancroft, J. C., Geiger, H. D., and Foltinek, D., 1994, Prestack migration by equivalent offset and CSP gathers: *CREWES Research Report*, **6**, 27.1–27.13.

Bancroft, J. C., Geiger, H., Wang, S., and Foltinek, D., 1995, Prestack migration by equivalent offset and CSP gathers: an update: *CREWES Research Report*, **7**, 27.1–27.10.

Bancroft, J. C., Geiger, H. D., and Margrave, G. F., 1998, The equivalent offset method of prestack time migration: *Geophysics*, **63**, 2042–2053. doi:10.1190/1.1444497

Dai, H., and Li, X.-Y., 2007, Velocity model updating in prestack Kirchhoff time migration for PS converted waves: Part I – Theory: *Geophysical Prospecting*, **55**, 525–547. doi:10.1111/j.1365-2478.2007.00629.x

Li, X. Y., and Bancroft, J. C., 1997, Converted wave migration and common conversion point binning by equivalent offset: *67th Annual International Management Social Exploration Geophysics Expanded Abstracts*, 1587–1590.

Wang, S., Bancroft, J. C., and Lawton, D. C., 1996, Converted-wave (P-SV) prestack migration and migration velocity analysis: *66th Annual International Management Social Exploration Geophysics Expanded Abstracts*, 1575–1578.

Wei, W., Junjie, Y., Xuewei, L., Junmeng, Z., Yun, W., and Ying, H., 2007, Equivalent offset method and its application: *Chinese Journal of Geophysics*, **50**, 1580–1587.

Appendix A

The following derivation refers completely to Bancroft et al. (1998), and the only different parameter is equivalent velocity V_e.

The DSR equation 3 is modified by resorting and moving the velocity to get

$$\left[\left(\frac{T_0V_e}{2}\right)^2+(x+h^2)\right]^{\frac{1}{2}}=2\left[\left(\frac{T_0V_e}{2}\right)^2+h_e^2\right]^{\frac{1}{2}}-\left[\left(\frac{T_0V_e}{2}\right)^2+(x-h)^2)\right]^{\frac{1}{2}}. \tag{A-1}$$

Then by squaring, we can get

$$\left(\frac{T_0V_e}{2}\right)^2+(x+h)^2=4\left[\left(\frac{T_0V_e}{2}\right)^2+h_e^2\right]+\left(\frac{T_0V_e}{2}\right)^2+(x-h)^2-4\left\{\left[\left(\frac{T_0V_e}{2}\right)^2+h_e^2\right]\left[\left(\frac{T_0V_e}{2}\right)^2+\left(x-h^2\right)^2\right]\right\}^{\frac{1}{2}}. \tag{A-2}$$

Expanding terms,

$$\left(\frac{T_0V_e}{2}\right)^2+x^2+h^2+2xh=4\left[\left(\frac{T_0V_e}{2}\right)^2+h_e^2\right]+\left(\frac{T_0V_e}{2}\right)^2+x^2+h^2-2xh-4\left\{\left[\left(\frac{T_0V_e}{2}\right)^2+h_e^2\right]\left[\left(\frac{T_0V_e}{2}\right)^2+(x-h)^2\right]\right\}^{\frac{1}{2}}. \tag{A-3}$$

to get

$$4xh=4\left[\left(\frac{T_0V_e}{2}\right)^2+h_e^2\right]-4\left\{\left[\left(\frac{T_0V_e}{2}\right)^2+h_e^2\right]\left[\left(\frac{T_0V_e}{2}\right)^2+(x-h)^2\right]\right\}^{\frac{1}{2}} \tag{A-4}$$

which then can be written as

$$\left[\left(\frac{T_0V_e}{2}\right)^2+(x-h)^2\right]^{\frac{1}{2}}=\left\{\left[\left(\frac{T_0V_e}{2}\right)^2+h_e^2\right]-xh\right\}/\left[\left(\frac{T_0V_e}{2}\right)^2+h_e^2\right]^{\frac{1}{2}}. \tag{A-5}$$

Simplifying

$$\left[\left(\frac{T_0V_e}{2}\right)^2+(x-h)^2\right]^{\frac{1}{2}}=\left[\left(\frac{T_0V_e}{2}\right)^2+h_e^2\right]^{\frac{1}{2}}-xh/\left[\left(\frac{T_0V_e}{2}\right)^2+h_e^2\right]^{\frac{1}{2}}. \tag{A-6}$$

After squaring, it can be written as

$$\left(\frac{T_0V_e}{2}\right)^2+(x-h)^2=\left(\frac{T_0V_e}{2}\right)^2+h_e^2+\frac{(xh)^2}{\left(\frac{T_0V_e}{2}\right)^2+h_e^2}-2xh. \tag{A-7}$$

Eliminating terms, equation A-7 is changed to

$$h_e^2=x^2+h^2-\frac{(xh)^2}{\left(\frac{T_0V_e}{2}\right)^2+h_e^2}. \tag{A-8}$$

By equation 2, there is the following equation:

$$T_{p+s}=2\left[\left(\frac{Z_0}{V_e}\right)^2+\frac{h_e^2}{V_e^2}\right]^{\frac{1}{2}}=2\left[\left(\frac{T_0}{2}\right)^2+\frac{h_e^2}{V_e^2}\right]^{\frac{1}{2}}. \tag{A-9}$$

Squaring and resorting, equation A-9 can be written as:

$$\frac{{T_{p+s}}^2V_e^2}{4}=\left(\frac{T_0V_e}{2}\right)^2+h_e^2. \tag{A-10}$$

Substituting equation A-10 into equation A-8 we get

$$h_e^2=x^2+h^2-\left(\frac{2xh}{TV_{\mathrm{e}}}\right)^2. \tag{A-11}$$